ADVANCED MATERIALS
www.advmat.de
Materials Views
www.MaterialsViews.com

Theory of Piezo-Phototronics for Light-Emitting Diodes

*Yan Zhang and Zhong Lin Wang**

Semiconductors, such as ZnO, GaN, InN, and CdS, are piezoelectric materials because the crystals have a non-central symmetric wurtzite structure. Recently, piezoelectric semiconductor nano/microwires have been used as fundamental building blocks for fabricating a series of novel nano/microdevices,[1–5] such as nanogenerators,[6–9] piezoelectric field effect transistors,[10,11] piezotronic logic devices,[12,13] and piezo-phototronic devices.[14,15] Typical piezoelectric wurtzite semiconductor materials are important optoelectronic materials for photon detectors, solar cells, and light emitting diodes (LEDs). With the extension of research in piezotronic theories and experiments, a new field of piezo-phototronics has been formed, which is to use the piezoelectric potential induced by stress for controlling/tuning photon emission by carrier generation, transport, and recombination.[2,16]

Take the *c*-axis of a grown ZnO nanowire as an example, applying a tensile strain along the nanowire induces piezoelectric charges at its two ends, forming a piezoelectric potential inside the nanowire. This potential tunes the Schottky barrier height or p–n junction built-in potential at the contact/interface, thus, the photon emission process can be effectively tuned by controlling the carrier generation, transport, and recombination characteristics by the externally applied strain.

Based on our previous theoretical work on both static and dynamic transport models, the piezopotential distribution and the dynamic transport properties of the carriers have been investigated for piezoelectric semiconductors.[17] In this paper, we present a fundamental theoretical framework of piezo-phototronics for understanding and quantifying photon generation and carrier transport behavior in LED devices. We first give some analytical data for a ZnO piezoelectric p–n junction LED under simplified conditions, which provides a clear physical picture for understanding the piezo-phototronics effect. Furthermore, using the numerical method developed previously for a piezotronic transistor,[17] the characteristics of a typical piezo-phototronic device and ZnO nanowire p–n junction LED are simulated by a finite element method (FEM). The theoretical results establish the basic physics for understanding the characteristics of piezo-phototronic devices and providing guidance for future device design.

Basic Principle of the Piezo-Phototronics Devices: Take a typical LED (**Figure 1**a) as an example, the basic structure is a p–n junction. There are excessive carriers over their equilibrium values under forward bias. Thus, radiative recombination will take place by injecting minority carriers. The same concepts can apply to a single semiconductor nanowire (NW) LED. The working principle of the LED is to use a forward bias to obtain a radiative recombination between electrons and holes at the junction.

A piezo-phototronic LED is assumed to be a p-type non-piezoelectric and n-type piezoelectric heterostructure junction, as shown in Figure 1b and c. The fundamental principle of the piezo-phototronic device is that piezoelectric charges created at the junction area significantly modify the band structure at the interface, resulting in control over the carrier generation, transport, and recombination at the p–n junction or metal–semiconductor interface.

Theoretical Frame of the Piezo-Phototronic Effect: Semiconductor physics and piezoelectric theories are used for describing the process involved in a piezo-phototronic device that is fabricated by a piezoelectric semiconductor. The static and dynamic transport behavior of the charge carriers and the interaction of a photon and an electron in semiconductors are described by semiconductor physics.[18] The behaviors of the piezoelectric material under dynamic straining are described by piezoelectric theories.[19] Therefore, electrostatic equations, current–density equations, continuity equations, and piezoelectric equations are applied as basic governing equations for characterizing piezo-phototronic devices.

The electrostatic behavior of charges in a piezoelectric semiconductor is described by the Poisson equation:

$$\nabla^2 \psi_i = -\frac{\rho(\vec{r})}{\varepsilon_s} \tag{1}$$

where ψ_i, $\rho(\vec{r})$ and ε_s are the electric potential distribution, the charge density distribution, and the permittivity of the material.

The drift and diffusion current density equations that correlate the local fields, charge densities, and local currents are:

$$\begin{cases} \mathbf{J_n} = q\mu_n n\mathbf{E} + qD_n \nabla n \\ \mathbf{J_p} = q\mu_p p\mathbf{E} - qD_p \nabla p \\ \mathbf{J} = \mathbf{J_n} + \mathbf{J_p} \end{cases} \tag{2}$$

where J_n and J_p are the electron and hole current densities, q is the absolute value of unit electronic charge, μ_n and μ_p are electron and hole mobilities, n and p are concentrations of free electrons and free holes, D_n and D_p are diffusion coefficients for electrons and holes, respectively, E is electric field, and J is the total current density.

The charge transport under the driving of a field is described by the continuity equations.

Dr. Y. Zhang, Prof. Z. L. Wang
School of Material Science and Engineering
Georgia Institute of Technology
Atlanta, Georgia 30332-0245, USA
E-mail: zlwang@gatech.edu

DOI: 10.1002/adma.201104263

© 2012 WILEY-VCH Verlag GmbH & Co. KGaA, Weinheim

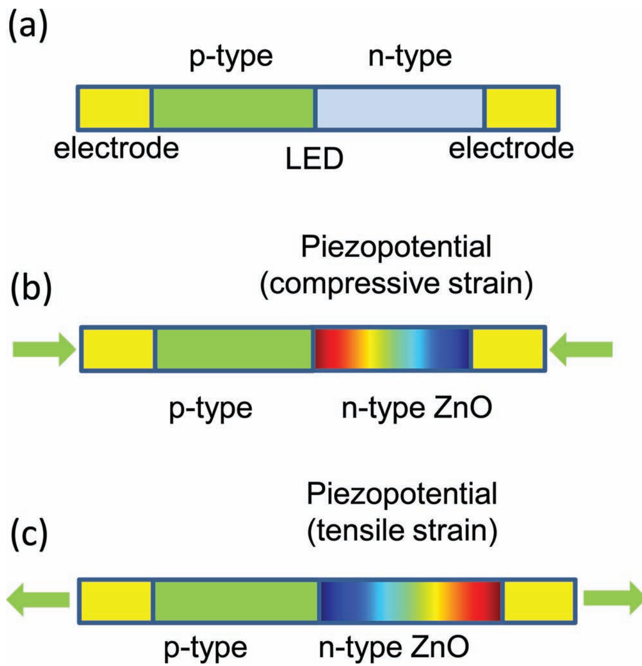

Figure 1. Schematic of a) a general n-type piezoelectric nanowire LED fabricated using a p–n heterojunction structure. Schematic of a piezo-phototronic device: piezo-LED under b) compressive and c)tensile strain, where the sign and magnitude of the piezopotential tunes/controls the photon emission, carrier generation, and transport characteristics. The color code represents the distribution of the piezopotential at the n-type nanowire. The red side has a higher piezopotential and the blue side is the low piezopotential side.

$$\begin{cases} \frac{\partial n}{\partial t} = G_n - U_n + \frac{1}{q}\nabla \cdot \mathbf{J_n} \\ \frac{\partial p}{\partial t} = G_p - U_p - \frac{1}{q}\nabla \cdot \mathbf{J_p} \end{cases} \quad (3)$$

where G_n and G_p are the electron and hole generation rates, and U_n and U_p are the recombination rates, respectively.

The relationship between the polarization and a small uniform mechanical strain S is given by:[19]

$$(\mathbf{P})_i = (\mathbf{e})_{ijk}(S)_{jk} \quad (4)$$

where the third order tensor $(\mathbf{e})_{ijk}$ is the piezoelectric tensor. The constituent equations can be written as:[19–21]

$$\begin{cases} \sigma = \mathbf{c_E S} - \mathbf{e^T E} \\ \mathbf{D} = \mathbf{eS} + \mathbf{kE} \end{cases} \quad (5)$$

where σ and $\mathbf{c_E}$ are the stress tensor and the elasticity tensor, respectively. E, D, and $\mathbf{k}$ are the electric field, the electric displacement, and the dielectric tensor, respectively.

Analysis of Piezo-Phototronic Effect for the Simplified Piezoelectric LED Case: The interaction of a photon and an electron in a semiconductor device has three main optical processes:[18] First, an electron excitation from the valence band to the conduction band may be induced by a photon absorption. This process is the dominant process for photodetectors and solar cells. Second, the reverse process of the above absorption named recombination is a photon emission induced by an electron returning from the conduction band to the valence band, which is the main process for LEDs. Third, an injected photon stimulates another similar photon by a recombination process and gives out two coherent photons.

In this paper, we take the LED as an example to present the piezo-phototronic effect. Vast literature exists about the experimental and theoretical study on the relationship between LED light intensity and applied current density for general application in display and optical communication. The LED light intensity is a non-linear relationship of the applied current density. The LED optical power density P_{optic} is a non-linear function of the current density J. Therefore, the linear relationship can be considered as the first order approximation. For simplicity, the LED optical power density P_{optic} with current density J can be generally considered as a power law relationship:

$$P_{\text{optic}} = \beta J^b \quad (6)$$

where β is a constant depending on device materials and structures, b is the power law parameter, with $b = 1$ corresponding to linear approximation and $b \neq 1$ a non-linear approximation. From our previous experimental works,[15] $b = 1.6$.

Figure 2 shows the change in band structure at a p–n junction with the presence of piezoelectric charges at the interface. The existence of the piezo-charges introduce three effects: a shift in local band as a result of the introduced local potential, a tilt of the band over the junction region for the polarization existing in the piezoelectric semiconductor, and a change in the charge depletion zone because of the redistribution of the local charge carriers to balance the local piezo-charges.

According to classical semiconductor physics[18] and our theoretical works about the piezotronics effect,[17] we take an ideal junction as an example to understand the piezo-phototronics effect. It must be mentioned that our previous model neglected the non-ideal factors, such as the size effect, surface effect, and non-uniform/non-homogeneous distribution of stress, etc. Therefore, we use the one-dimension model for the ideal p–n junction case, so the mechanism of the piezo-phototronic effect can also be applied to bulk and thin film materials. According to the depletion assumptions of the simplified analytical model,[17] the majority of carriers have been removed in the depletion region. Thus, we assumed the piezoelectric charges are not screened by carriers in the depletion region and distribute uniformly at the interface of the p–n junction within a width of W_{piezo}. In this ideal case, the direct current (DC) characteristics result from the energy band change induced by the piezoelectric charges. The energy band diagrams are shown for the piezoelectric LED in Figure 2a and b, the positive piezoelectric charges at the junction lower the energy band and the negative piezoelectric charges raise the energy band in the n-type semiconductor region near the junction region. For an n-type single-side abrupt junction with donor concentration N_D, and locally $p_{n0} >> n_{p0}$, the total current density had been received by solving the above basic Equations (1–5) for a piezotronic p–n junction:[17]

$$J = J_{C0} exp\left(\frac{q^2 \rho_{\text{piezo}} W_{\text{piezo}}^2}{2\varepsilon_s kT}\right)\left[exp\left(\frac{qV}{kT}\right) - 1\right] \quad (7)$$

where ρ_{piezo} is the density of polarization charges (in units of electron charge) and piezoelectric charges distribute at the

© 2012 WILEY-VCH Verlag GmbH & Co. KGaA, Weinheim

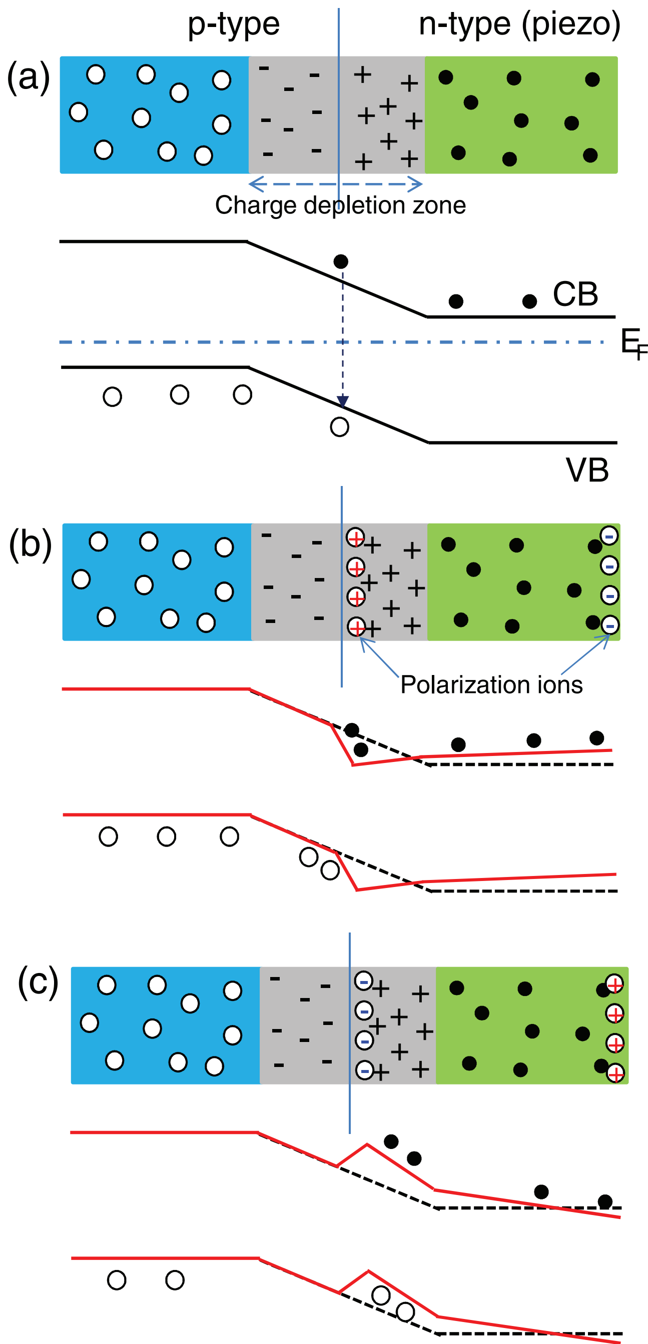

Figure 2. Energy band diagrams for a p–n junction a) with the absence of piezo-charges and b,c) with the presence of positive and negative piezo-charges at the junction, respectively. The red solid lines are the band diagrams when considering the piezopotential.

interface of the p–n junction within a width of W_{piezo}; the saturation current density and the Fermi level with the absence of piezopotential are defined by J_{C0} and E_{F0}:

$$J_{C0} = \frac{q D_p n_i}{L_p} \ exp\left(\frac{E_i - E_{F0}}{kT}\right) \tag{8}$$

where n_i and E_i are the intrinsic carrier density and the intrinsic Fermi level, respectively, and L_p is the diffusion length of holes.

According to Equations (6–8), the piezo-LED optical power output can be obtained as:

$$P_{optic} = \beta \left\{ J_{C0} \ exp\left(\frac{q^2 \rho_{piezo} W_{piezo}^2}{2\varepsilon_s kT}\right) \left[exp\left(\frac{qV}{kT}\right) - 1\right] \right\}^b \tag{9}$$

The efficiency of an LED is determined by: 1) the internal quantum efficiency, η_{in}, which is defined as the ratio of the number of photons emitted internally to the number of injected carriers passing the junction; 2) the optical efficiency, η_{op}; 3) the external quantum efficiency, η_{ex}; and 4) the power efficiency, η_P.[18]

For ease of comparison with experimental data, we calculate the external quantum efficiency for the simple cases described above as:

$$\eta_{ex} = N_{photons} / N_{elec} \tag{10}$$

where $N_{photons}$ and N_{elec} are the number of photons emitted externally and the number of carriers passing the junction, respectively. If P_{optic} is the optical power density received from the device per unit area, and J is the injection current density, the external quantum efficiency can be rewritten as:

$$\eta_{ex} = \frac{q \ P_{optic}}{h\nu \ J} \tag{11}$$

where $h\nu$ is the energy of the emitted photon. Thus, the external quantum efficiency can be rewritten as:

$$\eta_{ex} = \alpha \eta_{ex0} \tag{12}$$

where η_{ex0} is defined as the external quantum efficiency without piezoelectric charges inside the p–n junction:

$$\eta_{ex0} = \frac{\beta q}{h\nu} \left\{ J_{C0} \left[exp\left(\frac{qV}{kT}\right) - 1\right] \right\}^{b-1} \tag{13}$$

and α is defined as the factor representing the piezo-phototronics effect:

$$\alpha = \left\{ exp\left(\frac{q^2 \rho_{piezo} W_{piezo}^2}{2\varepsilon_s kT}\right) \right\}^{b-1} \tag{14}$$

which describes the ability of the piezoelectric charges to tune/control the carrier transport and photon recombination process.

According to Equation (9), it is obvious that the relationship between LED optical power density P_{optic} and current density J is non-linear. More importantly, Equations (9) and (13) show that not only LED optical power output but also the external quantum efficiency of the piezoelectric p–n junction LED have a non-linear relationship with local piezoelectric charges. Therefore, the photon emission process can be effectively tuned or controlled by not only the magnitude of the strain, but also the sign of the strain (tensile vs compressive). This is the mechanism of the piezo-phototronic devices for p–n junction LEDs.[15]

For GaN or ZnO nanowires grown along a c-axis, with a strain s_{33} along the c-axis, the piezocoefficient matrix is given by $(e)_{ijk} = \begin{pmatrix} 0 & 0 & 0 & 0 & e_{15} & 0 \\ 0 & 0 & 0 & e_{15} & 0 & 0 \\ e_{31} & e_{31} & e_{33} & 0 & 0 & 0 \end{pmatrix}$, the surface charge density σ and piezoelectric polarization can be obtained from Equation (4): $-\sigma = P_z = e_{33}s_{33}$. The compress and tensile strain are defined as negative and positive strain, respectively. Thus, $e_{33}s_{33} = -q\rho_{piezo} W_{piezo}$. We chose a typical non-linear

© 2012 WILEY-VCH Verlag GmbH & Co. KGaA, Weinheim

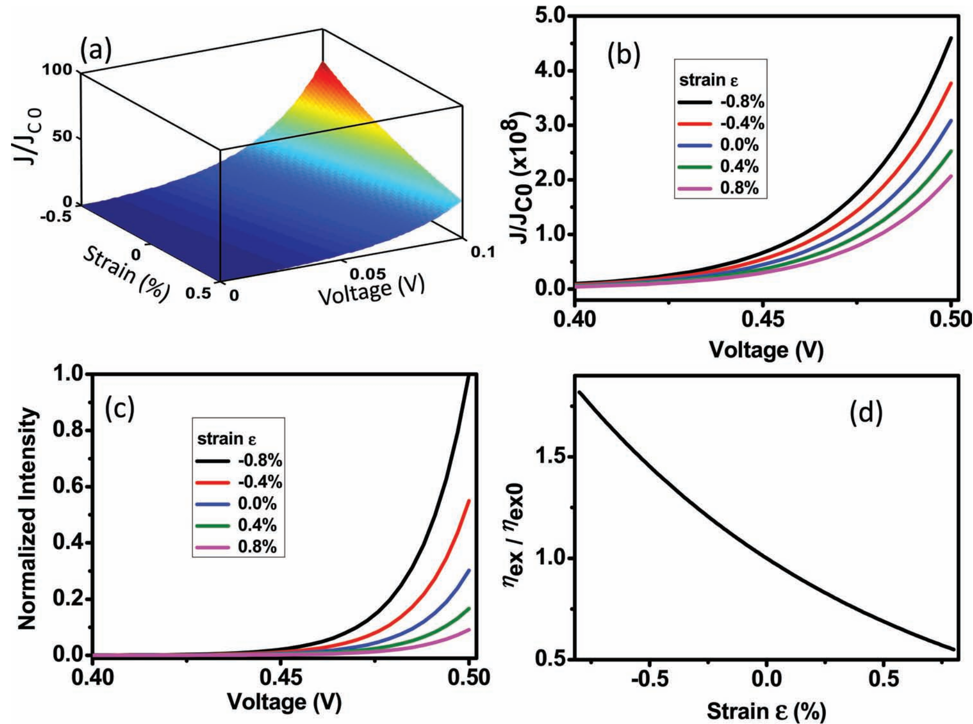

Figure 3. a) Calculated current–voltage characteristics of a piezo-LED with the presence of piezoelectric charges under various strain. b) Relative current density and c)relative light intensity as a function of applied voltage at various applied strain (–0.8% to 0.8%). d) Relative external quantum efficiency as a function of applied strain.

approximation, $b = 2$, thus the piezo-LED optical power output is given by:

$$P_{\text{optic}} = \beta\left\{J_{C0}\ exp\left(-\frac{q\,e_{33}\,s_{33}\,W_{\text{piezo}}}{2\varepsilon_s\,kT}\right)\left[exp\left(\frac{qV}{kT}\right)-1\right]\right\}^2 \tag{15}$$

Therefore, the external quantum efficiency can be obtained as:

$$\eta_{\text{ex}} = exp\left(-\frac{q\,e_{33}\,s_{33}\,W_{\text{piezo}}}{2\varepsilon_s\,kT}\right)\eta_{\text{ex0}} \tag{16}$$

The piezo-phototronics effect factor in this case is given by:

$$\alpha = exp\left(-\frac{q\,e_{33}\,s_{33}\,W_{\text{piezo}}}{2\varepsilon_s\,kT}\right) \tag{17}$$

According to Equations (15–17), the current density, relative light intensity, and the external quantum efficiency are calculated with typical material constants: piezoelectric constants $e_{33} = 1.22$ C m^{-2} and relative dielectric constant $\varepsilon_s = 8.91$. The width of the piezo-charges is $W_{\text{piezo}} = 0.25$ nm. The temperature is $T = 300$ K. Figure 3a shows the calculated J/J_{C0} as a function of the externally applied voltage V and applied strain. The DC characteristics of the piezoelectric LED with applied strain varied from –0.8% to 0.8% as shown in Figure 3b. When the strain changes from 0.8% to –0.8%, the light intensity increases by 1095% at $V = 0.5$ V in Figure 3c. Figure 3d shows the relative external quantum efficiency as a function of the externally applied strain, which clearly demonstrates piezoelectric tune/control on the photo emission process in the piezo-LED. This is the core physics of the piezo-phototronic effect.

Numerical Simulation of Piezoelectric p–n Junction LED Devices: The simplified analyses for one-dimensional cases provide qualitative guidance for understanding the mechanism of how the piezopotential tunes/controls the photon emission behavior. In the above simplified case, the non-radiative recombination is neglected for understanding the core of piezo-phototronics. According to our previous theoretical works about piezotronics,[17,22] the DC characteristics of the piezo p–n junction LED with strain can be numerically solved by Equations (1–5). We assume that the relationship between LED optical power density P_{optic} and current density J is $P_{\text{optic}} = \beta J^b$.

Using the numerical model which was developed for the piezoelectric p–n junction,[17] the piezoelectric equations, the electrostatic equation, and the convection and diffusion equations are solved with the piezoelectric charge distribution provided.

There are two recombination processes: band-to-band recombination process and trap-assisted recombination process (named Shockley–Read–Hall recombination). The radiative process (photon emission) relates to band-to-band recombination, in which the energy transfers from the conduction band to the valence band. The Shockley–Read–Hall recombination relates to the non-radiative process, which describes the recombination process by traps in the forbidden bandgap of the semiconductor. For simplicity, we neglect another non-radiative process, the Auger process, which is about the energy transfer from an injected electron or hole to another free electron or hole.

Following the piezoelectric diode model,[17] the electron and hole generation rates $G_n = G_p = 0$, which means no external optical excitation in our model. Using the method developed

© 2012 WILEY-VCH Verlag GmbH & Co. KGaA, Weinheim

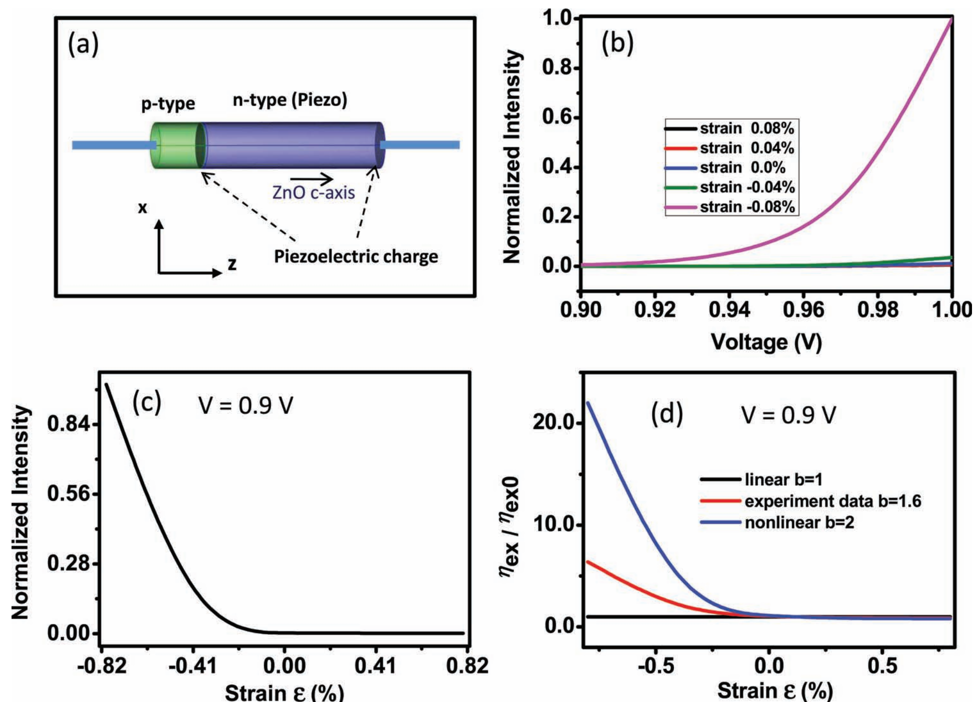

Figure 4. a) Schematic of a ZnO nanowire piezo-LED. b) Calculated relative intensity–voltage curves of the LED at various applied strain (–0.08% to 0.08%). c) Relative light intensity as a function of applied strain (–0.08% to 0.08%) at a fixed forward bias voltage of 0.9 V. d) Relative external quantum efficiency as a function of applied strain at a fixed forward bias voltage of 0.9 V with linear approximation, parabolic approximation, and fitting parameter from our previous experiments data.

in our previous work,[17] the dopant concentration N is approximately described using Gaussian functions, The n-type background doping concentration due to the presence of intrinsic defects is defined as N_{Dn}. The maximum donor and acceptor doping concentration are N_{Dnmax} and N_{Apmax}, respectively. We use ch to control the spread width of the dopant concentration. In our simulation, we choose n-type ZnO as the piezoelectric semiconductor material. The length and radius of the nanowire device are 100 and 10 nm, respectively. The length of the non-piezoelectric p-type is 20 nm and the length of n-type ZnO is 80 nm. The relative dielectric constants are $\kappa^r_\perp = 7.77$ and $\kappa^r_{//} = 8.91$. The intrinsic carrier density is $n_i = 1.0 \times 10^6$ cm^{-3}. The electron and hole mobilities are $\mu_n = 200$ cm^2 V^{-1} s^{-1} and $\mu_p = 180$ cm^2 V^{-1} s^{-1}. The carrier lifetimes are $\tau_p = 0.1$ µs and $\tau_n = 0.1$ µs. The n-type background doping concentration is $N_{Dn} = 1 \times 10^{15}$ cm^{-3}. The maximum donor doping concentration is $N_{Dnmax} = 1 \times 10^{17}$ cm^{-3} and the maximum acceptor doping concentration is $N_{Apmax} = 1 \times 10^{17}$ cm^{-3}. The control constant $ch = 4.66$ nm. The temperature is $T = 300$ K. The piezoelectric charges are assumed to distribute uniformly at the two ends of the n-type segment within a region of 0.25 nm in **Figure 4**a. For ease of labeling, a z-axis is defined in Figure 4a, where $z = 0$ represents the end of the p-type. The p–n junction is located at $z = 20$ nm along the axis. The n-type ends at $z = 100$ nm.

The intensity–voltage curves are shown under various strains at $b = 2$ in Figure 4b. According to piezotronics theory, positive local piezoelectric charges are created by the negative strain (compressive strain) in our model, which reduces the built-in potential of the p–n junction. Thus, the corresponding saturation current density increases. As a result, current density increases at a fixed bias voltage, which results in an increase of the light intensity. Alternatively, negative piezoelectric charges induced by the positive strain (tensile strain) increase the built-in potential and reduce the saturation current. Thus, the corresponding current density and light intensity decrease at a fixed bias voltage. In Figure 4c, the intensity shows a clear trend of change at various strains from –0.08% to 0.08% at a fixed voltage $V = 0.9$ V, apparently displaying the effect of piezoelectric charges on the photon emission. Using our model, we also studied the relative external quantum efficiency (piezo-phototronic factor α) at various strains at a fixed voltage $V = 0.9$ V. Figure 4d shows the relative external quantum efficiency (piezo-phototronic factor α) at various strains from –0.08% to 0.08%. By choosing the power law parameter $b = 1$, $b = 2$, and $b = 1.6$, the calculated piezo-phototronic factor and strain curves correspond to a linear approximation, a parabolic approximation (a typical non-linear approximation), and experimental fitted data, respectively.

For a comparison to the case shown in Figure 4a, we reverse the c-axis polarity of the n-type side (**Figure 5**a), or exchange the n and p segments (Figure 5c) as shown in the insets. The relative intensity and relative external quantum efficiency of the two cases are plotted in Figure 5a and b, respectively. In the case of Figure 5a in which the c-axis is pointing toward the p–n junction, the trend of relative intensity and the relative external quantum efficiency as shown in Figure 5a and Figure 5b is opposite to that shown in Figure 4c and 4d, because the sign of the piezoelectric charges is reversed.

© 2012 WILEY-VCH Verlag GmbH & Co. KGaA, Weinheim

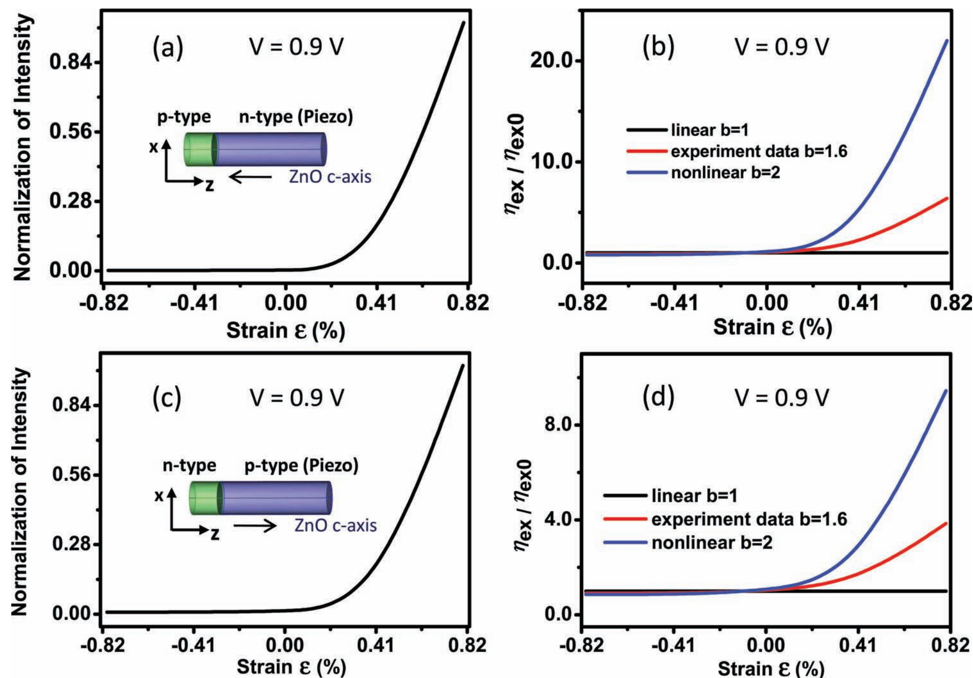

Figure 5. A ZnO nanowire piezo-LED with the n-side (ZnO) being piezoelectric and the *c*-axis pointing toward the junction. a) Relative light intensity and b) relative external quantum efficiency under linear approximation, parabolic approximation, and fitting parameter from our previous experimental data at a fixed forward bias voltage of 0.9 V under various applied strain (–0.08% to 0.08%). c) Relative light intensity and d) relative external quantum efficiency of a piezo-LED, with the p-side being piezoelectric and the c-axis pointing away from the junction. The insets are the corresponding schematics in (a) and (c).

For non-piezoeletric n-type material and piezoelectric p-type semiconductor piezoelectric LEDs, as shown in Figure 5c and d, the calculated relative intensity and relative external quantum efficiency show the same trend as for Figure 5a and b. The results indicate that a choice of n- or p-type piezoelectric semiconductor materials and their corresponding piezoelectric polar directions may be used for effectively tuning the output of the piezoelectric LED.

Therefore, the piezoelectric charges at the p–n interface dominate the photon emission process, in agreement with our experimental results.[15] The numerical results indicate that the piezo-phototronics effect is the result of tuning/controlling the light intensity and external quantum efficiency in the device by the generated piezoelectric charges inside the p–n junction.

Discussion: The results of the simplified analytical model provide semi-qualitative understanding about the mechanism of how the piezoelectric charges affect the DC characteristics of a piezoelectric LED. The numerical model demonstrates the basic method for simulating a piezoelectric p–n junction LED.[17] There are two main differences between the simplified analytical model and the numerical model in this paper: 1) The numerical model can apply to an arbitrary profile of the depletion layer. In this paper, the dopant concentration function *N* has been approximately described using Gaussian functions. In the simplified analytical model, it is assumed as a box profile.[18] 2) According to the depletion assumptions of the analytical model, the majority of carriers have been removed in the depletion region, thus, the piezo-charges inside the depletion region are not screened by carriers. Thus, the DC characteristics are tuned owing to the change in band structure by the piezo-charges. In comparison to our numerical model, both the energy band change and the carrier redistribution effect are included. Therefore, the numerical model gives much steeper curves than that of the simplified analytical model (see Figure 2d and Figure 3c). The main purpose of this manuscript is to develop a general theoretical approach about piezoelectric LEDs. Although the experimental system is the ZnO/GaN heterojunction given by Yang et al.,[15] the p–n junction model can be employed as a good approximation for qualitatively understanding our previous experiment,[15] due to the similar bandgap of ZnO and GaN. In general, the relationship between the LED light intensity and applied current density may depend on the different semiconductor materials and the different device structures, resulting in possible dependence of the power law parameter *b* in Equation (6) on the material properties and the device structures.

For simplifying the analysis, our analytical and numerical model neglected the size effect, this may affect the properties of materials at the nanometer scale, such as mechanical, electrical, thermal, and optical. An ideal one-dimension model is taken as an example for the ease of understanding the novel properties of piezo-phototronics devices, the presented methodology can be expanded to piezoelectric heterojunctions, which may have four possible configurations for experiment designs: a combination of two semiconductors (non-piezoelectric and piezoelectric material) and the two heterostructures (isotype and anisotype).[18] Furthermore, the presented methodology may also apply to the ferroelectric semiconductor materials,

© 2012 WILEY-VCH Verlag GmbH & Co. KGaA, Weinheim

COMMUNICATION

such as SbS and $BaTiO_3$,[23] which can be good candidates for piezo-phtotronics.

In summary, we have presented the theoretical frame of piezo-phototronics by studying the photon emission at a p–n junction with the presence of local piezoelectric charges. The analytical results under simplified conditions are derived for understanding the core physics of the piezo-phototronics devices, and numerical models are developed to illustrate the photon emission process and carrier's transport characteristics of the piezoelectric LED in a practical case. The theory presented here not only establishes the solid physical background of piezo-phototronics, but also provides theoretical support for guiding experimental design.

Acknowledgements

Research was supported by U.S. Department of Energy, Office of Basic Energy Sciences, Division of Materials Sciences and Engineering under Award DE-FG02-07ER46394, NSF (CMMI 0403671).

Received: November 7, 2011
Revised: January 15, 2012
Published online: March 19, 2012

[1] C. M. Lieber, Z. L. Wang, *MRS Bull.* **2007**, *32*, 99.
[2] Z. L. Wang, *Nano Today* **2010**, *5*, 540.
[3] Z. L. Wang, R. Yang, J. Zhou, Y. Qin, C. Xu, Y. Hu, S. Xu, *Mater. Sci. Eng. R* **2010**, *70*, 320.
[4] L. C. L. Y. Voon, M. Willatzen, *J. Appl. Phys.* **2011**, 109.
[5] Y. Yang, J. J. Qi, Q. L. Liao, H. F. Li, Y. S. Wang, L. D. Tang, Y. Zhang, Nanotechnology **2009**, *20*, 125201.
[6] Z. L. Wang, J. H. Song, Science **2006**, *312*, 242.
[7] X. D. Wang, J. H. Song, J. Liu, Z. L. Wang, *Science* **2007**, *316*, 102.
[8] Y. Qin, X. D. Wang, Z. L. Wang, *Nature* **2008**, *451*, 809.
[9] V. Dallacasa, F. Dallacasa, P. Di Sia, E. Scavetta, D. Tonelli, *J. Nanosci. Nanotechnol.* **2010**, *10*, 1043.
[10] X. D. Wang, J. Zhou, J. H. Song, J. Liu, N. S. Xu, Z. L. Wang, *Nano Lett.* **2006**, *6*, 2768.
[11] S.-S. Kwon, W.-K. Hong, G. Jo, J. Maeng, T.-W. Kim, S. Song, T. Lee, *Adv. Mater.* **2008**, *20*, 4557.
[12] N. Liu, G. Fang, W. Zeng, H. Zhou, H. Long, X. Zou, Y. Liu, X. Zhao, *Appl. Phys. Lett.* **2010**, *97*, 243504.
[13] W. Wu, Y. Wei, Z. L. Wang, *Adv. Mater.* **2010**, *22*, 4711.
[14] Y. F. Hu, Y. Zhang, Y. L. Chang, R. L. Snyder, Z. L. Wang, *ACS Nano* **2010**, *4*, 4220.
[15] Q. Yang, W. H. Wang, S. Xu, Z. L. Wang, *Nano Lett.* **2011**, *11*, 4012.
[16] F. Boxberg, N. Sondergaard, H. Q. Xu, *Nano Lett.* **2010**, *10*, 1108.
[17] Y. Zhang, Y. Liu, Z. L. Wang, *Adv. Mater.* **2011**, *23*, 3004.
[18] S. M. Sze, *Physics of Semiconductor Devices*, Vol. 2nd ed., Wiley, New York **1981**.
[19] T. Ikeda, *Fundamentals of Piezoelectricity*, Oxford University Press, Oxford, UK **1996**.
[20] G. A. Maugin, *Continuum Mechanics of Electromagnetic Solids*, North-Holland, Amsterdam **1988**.
[21] R. W. Soutas-Little, *Elasticity, XVI, 431*, Dover Publications, Mineola, NY **1999**.
[22] *Comsol Model Gallery (Semiconductor Diode)*, http://www.comsol.com/showroom/gallery/114/ (last accessed Oct. 2011).
[23] J. W. Bennett, I. Grinberg, A. M. Rappe, *J. Am. Chem. Soc.* **2008**, *130*, 17409.

© 2012 WILEY-VCH Verlag GmbH & Co. KGaA, Weinheim